Optical Engineering 45(4), 043604 (April 2006)

Two-dimensional small-rotation-angle measurement using an imaging method

Takamasa Suzuki, MEMBER SPIE
Takanori Endo
Osami Sasaki, MEMBER SPIE
Niigata University
Faculty of Engineering
8050 Ikarashi 2
Niigata 950-2181, Japan
E-mail: takamasa@eng.niigata-u.ac.jp

John E. Greivenkamp, FELLOW SPIE
University of Arizona
Optical Sciences Center
Tucson, Arizona 85721

Abstract. A two-dimensional small-rotation-angle measurement system based on fringe projection is proposed and demonstrated. Simple and effective signal processing is described and applied to the angular calculation. Several measurements indicate a measurement accuracy of ≈0.4 arcsec, which is comparable to that of a high-priced autocollimator. The two-dimensional two-pitch grating used in our prototype system provides a wide measurement range, which is expected to reach 1300 arcsec for both *x*- and *y*-direction rotations. © *2006 Society of Photo-Optical Instrumentation Engineers.* [DOI: 10.1117/1.2188945]

Subject terms: rotation-angle measurement; fringe projection; two-dimensional grating; Fourier transform method.

Paper 050457R received Jun. 7, 2005; revised manuscript received Aug. 12, 2005; accepted for publication Aug. 16, 2005; published online Apr. 4, 2006.

1 Introduction

A lot of optical methods for angular measurement have been proposed to date. Those techniques are necessary to align machine tools, position mask wafers for integrated circuits, and so on. The autocollimator and the interferometer are well established devices for angular measurement. The former, while simple in structure, is expensive and not suitable for automatic on-line measurement, because it takes much time to align the measurement axis. Also, its measurement range is small. The latter, which is based on the interference of optical waves, converts the angular displacement into an optical path difference.[1] Many techniques have been proposed to improve the accuracy of such systems and to miniaturize them.

We have proposed several interferometers that measure small rotation angles by using parallel interference patterns (PIPs)[2] and sinusoidal phase modulation.[3] Orthogonal PIPs and paired PIPs have enabled two-dimensional[4] and wide-range[5] rotation-angle measurement, respectively, by eliminating external disturbance. Although these systems are able to realize highly accurate and wide-range rotation-angle measurement, they are complicated and large. Other techniques that simplify and miniaturize the interferometer have been proposed.[6–12] In such systems, at least one measurement arm in the interferometer contains prisms. Internal reflection in the prism yields a simple setup, cheapness, and high resolution. The measurement, however, suffers from external disturbance, because it uses interference of optical waves. Furthermore, it is difficult to extend the system to two-dimensional (2-D) measurement.

Another method, which is not based on interference but on internal reflection, has been developed.[13–15] While the system is compact and highly accurate, it also is restricted to one-dimensional (1-D) measurement.

The moiré technique is also useful to measure angular displacement.[16–18] It is applied to the mask aligner for semiconductor processing. The system is rather simple and cheap. It requires, however, a fine and precise 1-D grating, which results in restriction to 1-D measurement.

In this paper, we propose another type of technique for rotation-angle measurement. Because the measurement is not implemented by interference but by fringe projection, it is basically robust to external disturbance and simple in setup. Although the basic principle is the same as that of our previous system,[19] the configuration, signal processing, and performance are much improved. In particular, no reference mirror is required, and size of the object mirror is much reduced. In the signal processing, a highly efficient algorithm is introduced for the determination of a phase difference. The performance is especially improved in regard to the realization of 2-D measurement and high angular resolution. Several measurements and evaluations indicate that the measurement accuracy is ≈0.4 arcsec, which is ten times better than that in our previous system and is comparable to that of a high-priced autocollimator. Also, the measurement range has been expanded to ≈1300 arcsec for 2-D rotation-angle measurement by means of the projection of a two-pitch grating image.

2 Principle

2.1 *2-D Rotation-Angle Measurement*

Our system measures the angular displacements of the object mirror (M_O), which rotates around the *x*- and *y* axes. The principle of the measurement is illustrated in Fig. 1. The focal length of the imaging lens L is f_L. We used two kinds of 2-D grating in the experiments, which are illustrated in Fig. 2. We call them S1 and S2, respectively, in this paper. As shown in Fig. 2(a), S1 is a simple square grating whose pitches are p_x and p_y. On the other hand, S2 is divided into four sections. Each section is distinguished by referring to the segments p, q, r, and s as shown in Fig. 2(b). The pair of gratings in the areas p-r and q-s have the same pitches p_{x1} and p_{y1}. The other pair in the areas p-s and q-r have the same pitches p_{x2} and p_{y2}. That is, diagonally opposite pairs of gratings have the same pitch.

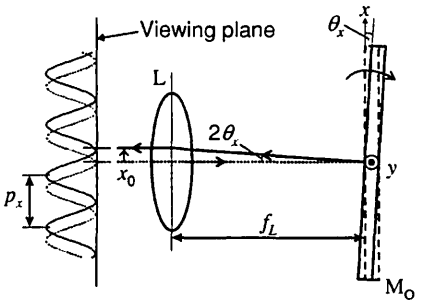

Fig. 1 Principle of the measurement: M_O, object mirror; L, imaging lens; x_0, fringe shift; p_x, pitch of the grating; f_L, focal length of the imaging lens.

Although the system possesses a 2-D grating as indicated in Fig. 2, we focus our attention on angular measurement around the y axis (in the x direction) to simplify the explanation, in which grating S1 is assumed. The grating image is focused onto M_O by lens L as shown in Fig. 1. The image is reflected to and observed on the viewing plane. We use the image that is captured before the mirror's rotation as the reference. If M_O rotates slightly by θ_x, the viewed image shifts by

$$x_0 = f_L \tan 2\theta_x \tag{1}$$

with respect to the reference image. We call the shifted image used for the angular-displacement measurement the *object image*. The rotation angle θ_x is then given by

$$\theta_x = \frac{1}{2}\tan^{-1}\left(\frac{x_0}{f_L}\right) \tag{2}$$

from Eq. (1). The shift x_0 is calculated from the phase difference between the reference and the object image. If we denote the reference and the object image as $g_1(x)$ and $g_2(x)$, respectively, they are expressed as

$$g_k(x) = a(x) + b(x)\cos\left(\frac{2\pi}{p_x}x + \phi_k\right) \qquad (k = 1,2), \tag{3}$$

where $a(x)$, $b(x)$, and ϕ_k are the background intensity, amplitude of the viewed grating image, and phases that are used for the rotation-angle calculation, respectively. We assume that $a(x)$ and $b(x)$ do not change with the shift of the grating. The shift x_0 can be calculated by

$$x_0 = \frac{p_x}{2\pi}\Delta\phi_x, \tag{4}$$

where $\Delta\phi_x = \phi_2 - \phi_1$ is the phase difference between $g_1(x)$ and $g_2(x)$. Substituting Eq. (4) into Eq. (2), we have the rotation angle

$$\theta_x = \frac{1}{2}\tan^{-1}\left(\frac{p_x}{2\pi f_L}\Delta\phi_x\right) \tag{5}$$

for the x direction. In the same way, the rotation angle for the y direction is given by

$$\theta_y = \frac{1}{2}\tan^{-1}\left(\frac{p_y}{2\pi f_L}\Delta\phi_y\right), \tag{6}$$

where $\Delta\phi_y$ is the phase difference between the reference and the object grating images in the y direction.

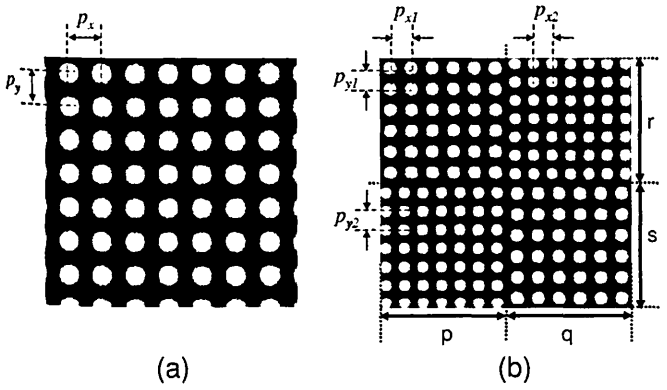

Fig. 2 Grating images (a) S1 of the 1-D grating and (b) S2 of the 2-D grating used in the experiments. S2 is divided into four sections.

2.2 *Signal Processing for the Determination of the Phase Difference*

In our system, the determination of the phase difference between $g_1(x)$ and $g_2(x)$ is the most important. In our previous paper,[19] the phase difference was obtained after detecting the phases of the reference and the object image by applying the Fourier transform (FT) method.[20] The FT method, however, uses both the FT and the inverse FT to obtain one phase. It requires a long calculating time. On the other hand, the signal processing we describe in this paper uses only the FT, it is very simple, and its calculating time is much shorter than that of the previous one.

We describe the process only for the x direction, to simplify the explanation. The grating images expressed in Eq. (3) are rewritten as follows:

$$g_k(x) = a(x) + c_k(x)\exp\left(i\frac{2\pi}{p_x}x\right) + c_k^*(x)\exp\left(-i\frac{2\pi}{p_x}x\right) \qquad (k=1,2), \tag{7}$$

where

$$c_k(x) = \frac{1}{2}b(x)\exp(i\phi_k), \tag{8}$$

and * denotes a complex conjugate. When the FT is applied to $g_k(x)$, we have

$$G_k(f) = A(f) + C_k\left(f - \frac{1}{p_x}\right) + C_k^*\left(f + \frac{1}{p_x}\right), \tag{9}$$

where capital letters denote the corresponding FTs. The Fourier spectra of $G_1(f)$ and $G_2(f)$ are separated on the frequency plane as illustrated in Fig. 3.

We now turn our attention to the Fourier spectra C_1^* and C_2 that are enclosed in the dashed rectangles in Fig. 3. If

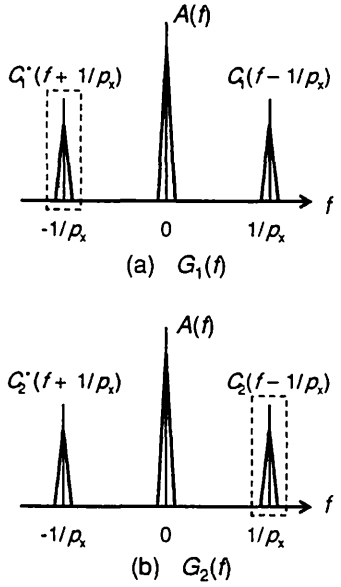

Fig. 3 Distribution of the Fourier spectra of (a) $G_1(f)$ and (b) $G_2(f)$. The phase difference is calculated by using the components enclosed in the dashed rectangles.

we extract those particular components from C_1^* and C_2 at $-1/p_x$ and $1/p_x$, respectively, they are given by

$$C_1^*(0) = \frac{1}{2}B^*(0)\exp(-i\phi_1) \tag{10}$$

and

$$C_2(0) = \frac{1}{2}B(0)\exp(i\phi_2), \tag{11}$$

where $B(f)$ is the FT of $b(x)$. Because the product of $C_1^*(0)$ and $C_2(0)$ is

$$C_1^*(0)C_2(0) = \frac{1}{4}|B(0)|^2\exp[i(\phi_2 - \phi_1)], \tag{12}$$

the phase difference is given by

$$\Delta\phi_x = \tan^{-1}\left\{\frac{\mathrm{Im}[C_1^*(0)C_2(0)]}{\mathrm{Re}[C_1^*(0)C_2(0)]}\right\}. \tag{13}$$

Thus we do not need to calculate ϕ_1 and ϕ_2, but can calculate $\Delta\phi_x$ directly without the inverse FT. The phase difference $\Delta\phi_y$ for the y direction can be calculated in a similar way.

Because $\Delta\phi_x$ and $\Delta\phi_y$ are confined to the region between 0 and 2π, the maximum measurable ranges for the x and the y direction are simply given by

$$\theta_{x\,\max} = \frac{1}{2}\tan^{-1}\left(\frac{p_x}{f_L}\right) \tag{14}$$

and

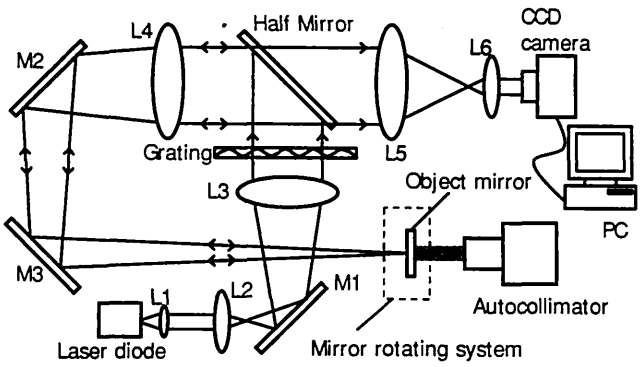

Fig. 4 Experimental setup: L, lenses; M, mirrors; PC, computer.

$$\theta_{y\,\max} = \frac{1}{2}\tan^{-1}\left(\frac{p_y}{f_L}\right), \tag{15}$$

respectively.

2.3 *Two-Pitch Method Modified for 2-D Measurement*

When $\Delta\phi_x$ and/or $\Delta\phi_y$ increase beyond 2π because of a large rotation of the mirror, an ambiguity occurs in the measurement. To eliminate this problem, we apply the two-pitch method[19] by use of S2. This is a technique similar to the traditional two-wavelength interferometry.[21] When we apply the two-pitch method for the x direction, we first exchange the areas q-r and q-s of the captured grating image before the phase analysis, whereas in the case of the y direction, the areas p-s and q-s must be exchanged. These processes allow us to increase the cycle numbers of the grating and to improve the measurement accuracy.[19] The principle of the 1-D two-pitch method is described in Ref. 19 in detail; here let us explain it briefly for the case of the 2-D measurement. If we use two pitches p_{x1} and p_{x2} after capturing the image of S2, the actual phase differences are represented by

$$\Delta\tilde{\phi}_{x1} = \Delta\phi_{x1} + 2m_x\pi \tag{16}$$

and

$$\Delta\tilde{\phi}_{x2} = \Delta\phi_{x2} + 2n_x\pi, \tag{17}$$

where $\Delta\phi_{x1}$ and $\Delta\phi_{x2}$ are the detectable phase differences for p_{x1} and p_{x2}, respectively, and m_x and n_x are integers. Assuming that $m_x = n_x$, they are given by

$$m_x = n_x = \mathrm{INT}\left[\frac{R_x\Delta\phi_{xs} - \Delta\phi_{x1}}{2\pi}\right], \tag{18}$$

where $R_x = p_{xs}/p_{x1}$ is the ratio between the synthetic grating pitch

$$p_{xs} = \frac{p_{x1}p_{x2}}{|p_{x1} - p_{x2}|} \tag{19}$$

for the x-direction and the original one, $\Delta\phi_{xs} = \Delta\phi_{x1} - \Delta\phi_{x2}$ is the difference between the detectable phase differences for the x direction, and the function INT[ ] gives the integer part of the argument. Substituting Eq. (18) into

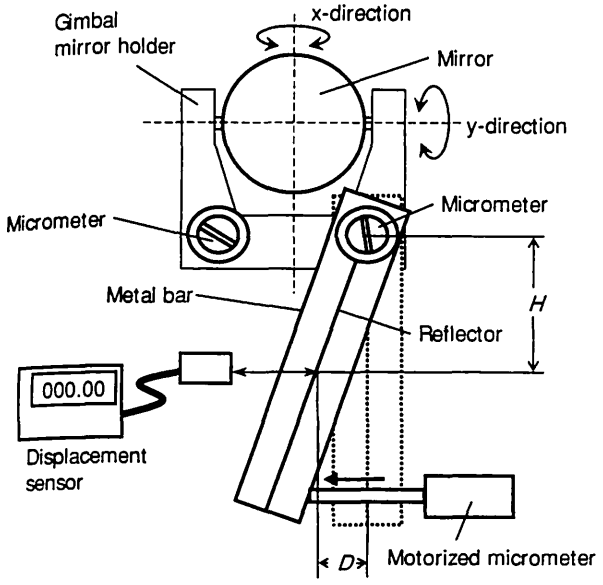

Fig. 5 Schematic of the mirror-rotating system.

Eq. (16), the actual phase difference $\Delta\tilde{\phi}_{x1}$ is obtained. Similar equations

$$\Delta\tilde{\phi}_{y1} = \Delta\phi_{y1} + 2m_y\pi, \tag{20}$$

$$\Delta\tilde{\phi}_{y2} = \Delta\phi_{y2} + 2n_y\pi, \tag{21}$$

$$m_y = n_y = \mathrm{INT}\left[\frac{R_y\,\Delta\phi_{ys} - \Delta\phi_{y1}}{2\pi}\right], \tag{22}$$

and

$$p_{ys} = \frac{p_{y1}p_{y2}}{|p_{y1} - p_{y2}|} \tag{23}$$

are derived for the y direction, where $\Delta\phi_{y1}$ and $\Delta\phi_{y2}$ are the detectable phase differences for p_{y1} and p_{y2}, respectively, $R_y = p_{ys}/p_{y1}$, and $\Delta\phi_{ys} = \Delta\phi_{y1} - \Delta\phi_{y2}$. The difference $\Delta\tilde{\phi}_{y1}$ is then calculated from Eqs. (20) and (22). Permuting $\Delta\tilde{\phi}_{x1}$ and $\Delta\tilde{\phi}_{y1}$ with $\Delta\phi_{x1}$ and $\Delta\phi_{y1}$ in Eqs. (5) and (6), respectively, 2-D rotation-angle measurement can be achieved over a wide range.

3 Experimental Setup

A schematic of the experimental setup is shown in Fig. 4. A compact laser diode (Hitachi HL6335), whose wavelength and output power are 635 nm and 5 mW, respectively, is used as a light source. The grating is irradiated by the light, and its image is focused onto the object mirror in the mirror-rotating system. The pitches of the gratings used in our experiments are $p_x = p_y = 1.7$ mm for S1, and $p_{x1} = p_{y1} = p_1 = 1.7$ mm and $p_{x2} = p_{y2} = p_2 = 1.5$ mm for S2. They were printed on a transparency with a laser-beam printer whose resolution was 600 dots/in. The focal length of the imaging lens L4 is $f_L = 1000$ mm. The grating image reflected by the mirror backpropagates and passes the half mirror. The CCD camera captures the image, which is shifted by the rotation of the mirror. The pixel number and the pitch of the CCD camera are 768×494 pixels and 6.4×7.5 μm, respectively. The captured images are processed by the computer in the frequency domain to calculate the rotation angle. At the same time, the rotation angle is measured by the autocollimator (Taylor-Hobson DA20) so as to estimate the accuracy of our system. The resolution and the measurable range of the DA20 are ±0.2 and ±20 arcsec, respectively.

The mirror-rotating system is illustrated in Fig. 5. A gimbal mirror holder is used to hold and rotate the object mirror. The angle of the mirror is controlled by rotating the two micrometers installed in the mirror holder. The angles change by $\beta_x = 0.68$ deg per turn and $\beta_y = 0.54$ deg per turn, respectively, for the x and the y direction. We attached the

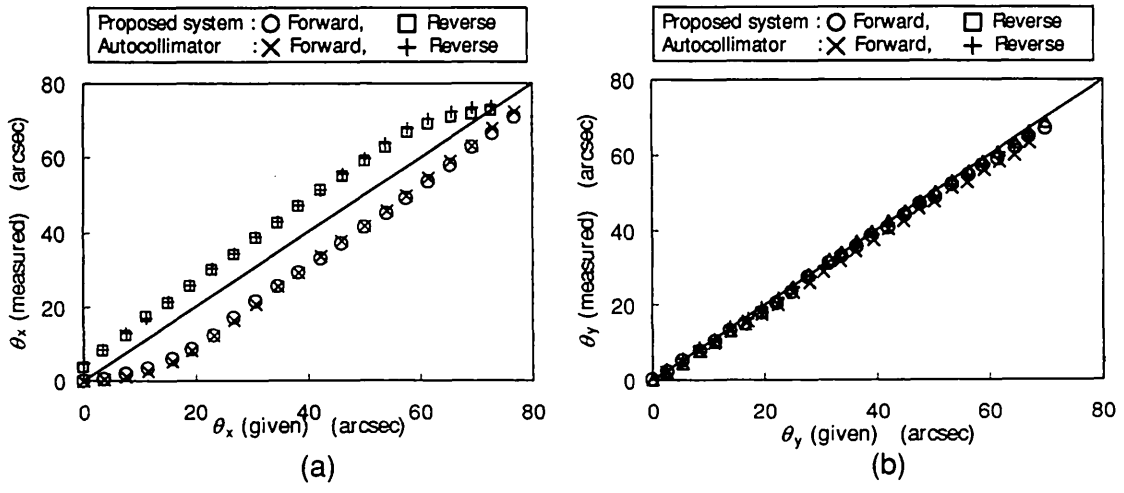

Fig. 6 Measured rotation angle for (a) the x direction and (b) the y direction in the range of 0 to 80 arcsec. "Forward" and "Reverse" mean increment and decrement of the angular displacement.

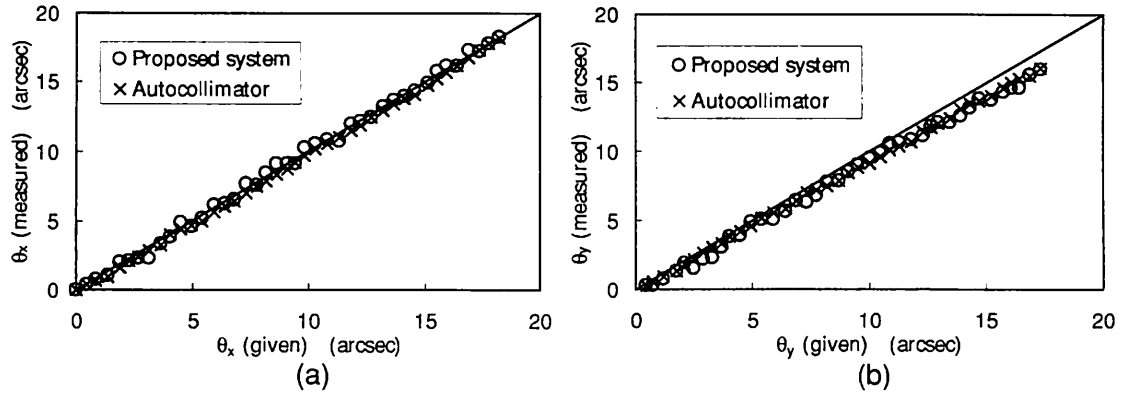

Fig. 7 Measured rotation angle for (a) the x direction and (b) the y direction in the range of 0 to 20 arcsec. The measurement was made in the "Forward" direction.

metal bar to one of the micrometers and moved it with the motorized micrometer head. The micrometer head was positioned at the end of the metal bar. We used a dedicated laser sensor whose resolution is 0.1 μm to monitor the displacement of the metal bar. The reflector attached to the metal bar reflects the sensor beam. The displacement D is monitored by the sensor at a distance H of 11 mm. The angles of rotation driven by the micrometer heads are given by

$$\theta_x = \frac{\beta_x}{2\pi} \tan^{-1}\left(\frac{D}{H}\right) \tag{24}$$

and

$$\theta_y = \frac{\beta_y}{2\pi} \tan^{-1}\left(\frac{D}{H}\right), \tag{25}$$

respectively. Although the rotation angle can be confirmed precisely by the autocollimator, we can estimate it roughly by monitoring D.

4 Results

We measured the rotation angles by using grating S1 to confirm the performance of the proposed system. From Eqs. (14) and (15), the maximum measurable ranges of the angular displacement are calculated as 175.3 arcsec for both directions. Figure 6 shows the measurement results, in which "Forward" and "Reverse" mean increment and decrement of the angular displacement, respectively. The solid lines in Fig. 6(a) and 6(b) show a slope of 45 deg. The "given" angles were calculated by using Eqs. (24) and (25). The angle was measured at intervals of ≈4 and ≈3 arcsec for the x and the y direction, respectively, by using our system and the autocollimator. While a large hysteresis loop is observed in Fig. 6(a), the results obtained by our system and by the autocollimator agreed very well. Because a lot of experiments had been made only for the x direction rotation, the screw of the micrometer could have been worn down. It seems likely that the hysteresis comes from this wear. We presume to show this result because the nonlinear change well confirms the measurement performance. The measurement results plotted in Fig. 6(b) show the linear dependence on the rotation angle that is given by the mirror-rotating system. The angles measured with our system and the autocollimator agreed well also in the y direction.

In these experiments, angular displacement was measured in the range of 0 to 80 arcsec, but we finely measured the rotation angle in the narrow range of 0 to 20 arcsec for the x and y directions to confirm the measurement error. The angle was measured every

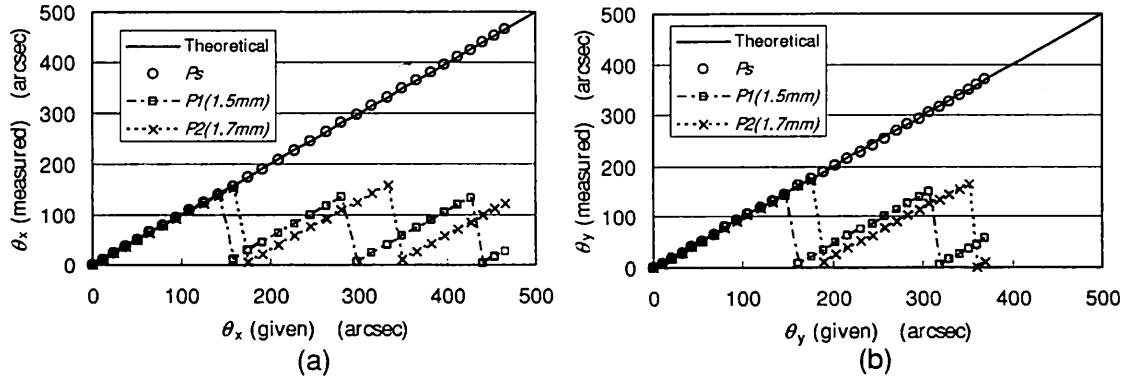

Fig. 8 Rotation angles for (a) the x direction and (b) the y direction measured with two-pitch grating S2. Plots on the dot-dash line and dotted line are obtained with a single pitch. Plots on the solid line are obtained by the two-pitch method.

≈1 arcsec for the "Forward" direction by use of our system and the autocollimator. Measurement for the x direction was made in the linear regions in Fig. 6(a), avoiding the nonlinear range. Results are shown in Fig. 7(a) and 7(b), respectively, for the x and the y direction. No major differences were found between the results obtained by our system and by the autocollimator. The differences between the measurement results obtained by the two devices are found to be 0.35 and 0.34 arcsec rms for the x and the y direction, respectively. These results allow us to estimate a measurement accuracy of ≈0.4 arcsec.

Next, we tried applying the 2-D two-pitch method by using S2. Although the maximum measurable ranges are estimated as 175.3 and 154.7 arcsec for p_1 and p_2, respectively, from Eqs. (14) and (15), it is expected that the measurement ranges for the both directions can be expanded up to ≈1314 arcsec, because the synthetic pitch is $p_{xs}=p_{ys}=p_s=12.75$ mm. Results obtained with S2 are shown in Fig. 8. In the x direction, measurements were conducted 30 times every ≈15 arcsec for p_1 and for p_2, as shown in Fig. 8(a). As we expected, the results obtained for p_1 and p_2 were discontinuous at ≈175 and ≈155 arcsec, respectively; but the rotation angle was measured without such discontinuities over the whole range when the two-pitch method was applied. The continuous plots agreed well with the theoretical line. The deviation from the theoretical line was 0.79 arcsec rms for the x direction. The same experiment was performed in the y direction. The angular displacement was measured every ≈12 arcsec for the y direction. Because the coefficient β_y is smaller than β_x, while every displacement of the metal bar driven by the motorized micrometer was the same for the x and the y direction, an angular displacement in the y direction was smaller than one in the x direction. Although the results obtained by p_1 and p_2 were discontinuous as shown in Fig. 8(b), the two-pitch method allowed us to compensate the discontinuity. The deviation from the theoretical line was 0.48 arcsec rms for the y direction.

5 Conclusion

We have proposed and demonstrated a small-rotation-angle measurement system that has wide measurement range. A precise two-dimensional measurement scheme was realized with a simple setup. Although the system proposed in this paper is a modification of our previous one, the configuration, the signal processing, and the performance are much improved. The laser light enables us to focus the beam on the object mirror, and it removes the requirement on the size of the object mirror. A simple and highly efficient signal processing scheme was proposed for calculating the phase difference. Several measurements confirmed that the measurement accuracy is ≈0.4 arcsec in our proposed system. The performance matched a high-priced autocollimator in accuracy. The two-pitch method enabled us to expand the measurement range. In our prototype, it covers the range from 0 to 1314 arcsec, which is superior to an autocollimator.

References

1. D. Malacara and O. Harris, "Interferometric measurement of angles," *Appl. Opt.* 9(7), 1630–1633 (1970).
2. X. Dai, O. Sasaki, J. E. Greivenkamp, and T. Suzuki, "Measurement of small rotation angles by using a parallel interference pattern," *Appl. Opt.* 34(28), 6380–6388 (1995).
3. O. Sasaki, C. Togashi, and T. Suzuki, "Two-dimensional rotation angle measurement using a sinusoidal phase-modulating laser diode interferometer," *Opt. Eng.* 42(4), 1132–1136 (2003).
4. X. Dai, O. Sasaki, J. E. Greivenkamp, and T. Suzuki, "Measurement of two-dimensional small rotation angles by using orthogonal parallel interference patterns," *Appl. Opt.* 35(28), 5657–5666 (1996).
5. X. Dai, O. Sasaki, J. E. Greivenkamp, and T. Suzuki, "High accuracy, wide range, rotation angle measurement by the use of parallel interference patterns," *Appl. Opt.* 36(25), 6190–6195 (1997).
6. J. Rohlin, "An interferometer for precision angle measurements," *Appl. Opt.* 2(7), 762–763 (1963).
7. P. Shi and E. Stijns, "New optical method for measuring small-angle rotations," *Appl. Opt.* 27(20), 4342–4344 (1988).
8. P. Shi and E. Stijns, "Improving the linearity of the Michelson interferometric angular measurement by a parameter compensation method," *Appl. Opt.* 32(1), 44–51 (1993).
9. M.-H. Chiu and D.-C. Su, "Improved technique for measuring small angles," *Appl. Opt.* 36(28), 7104–7106 (1993).
10. W. Zhou and L. Cai, "Interferometer for small-angle measurement based on total internal reflection," *Appl. Opt.* 37(25), 5957–5963 (1998).
11. W. Zhou and L. Cai, "Improved angle interferometer based on total internal reflection," *Appl. Opt.* 38(7), 1179–1185 (1999).
12. M. Ikram and G. Hussain, "Michelson interferometer for precision angle measurement," *Appl. Opt.* 38(1), 113–120 (1999).
13. P. S. Huang, S. Kiyono, and O. Kamada, "Angle measurement based on the internal-reflection effect: a new method," *Appl. Opt.* 31(28), 6047–6055 (1992).
14. P. S. Huang and J. Ni, "Angle measurement based on the internal-reflection effect and the use of right-angle prisms," *Appl. Opt.* 34(22), 4976–4981 (1995).
15. P. S. Huang and J. Ni, "Angle measurement based on the internal-reflection effect using elongated critical-angle prisms," *Appl. Opt.* 35(13), 2239–2241 (1996).
16. B. P. Singh, K. Varadan, and V. T. Chitnis, "Measurement of small angular displacement by a modified moiré technique," *Opt. Eng.* 31(12), 2665–2667 (1992).
17. B. P. Singh, T. Goto, R. Sharma, A. K. Kanjilal, R. Narain, V. T. Chitnis, J. Liu, and Y. Uchida, "Tracking and dynamic control of the angular alignment position in a photolithographic mask aligner by the moiré interference technique," *Rev. Sci. Instrum.* 66(3), 2658–2660 (1995).
18. J. Liu, H. Furuhashi, A. Torii, R. Sharma, V. T. Chitnis, B. P. Singh, J. Yamada, and Y. Uchida, "Automatic mask alignment in the θ direction using moiré sensors," *Nanotechnology* 6, 135–138 (1995).
19. T. Suzuki, H. Nakamura, and O. Sasaki, "Small-rotation-angle measurement using an imaging method," *Opt. Eng.* 40(3), 426–432 (2001).
20. M. Takeda, H. Ina, and S. Kobayashi, "Fourier-transform method of fringe-pattern analysis for computer-based topography and interferometry," *J. Opt. Soc. Am.* 72(1), 156–160 (1982).
21. C. Polhemus, "Two-wavelength interferometry," *Appl. Opt.* 12(9), 2071–2074 (1973).

Takamasa Suzuki received his BE and ME degrees in electrical engineering from Niigata University in 1982 and from Tohoku University in 1984, respectively, and his PhD degree in electrical engineering from Tokyo Institute of Technology in 1994. He is an associate professor of electrical and electronic engineering at Niigata University. His research interests include optical metrology and optical information processing.

Takanori Endo received his BE and ME degrees in electrical engineering from Niigata University in 2004 and 2006,, respectively. He is currently with the research staff of Canon Inc. When this paper was accepted, he was a master's course student in the Graduate School of Science and Technology at Niigata University. His research interest involves optical metrology. He currently engages in a study on wavelength scanning interferometry.

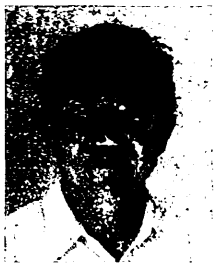

Osami Sasaki received his BE and ME degrees in electrical engineering from Niigata University in 1972 and 1974, respectively, and his PhD degree in electrical engineering from Tokyo Institute of Technology in 1981. He is a professor of electrical and electronic engineering at the Niigata University, and since 1974 he has worked in the field of optical measuring systems and optical information processing.

John E. Greivenkamp is a professor of optical sciences and ophthalmology at the University of Arizona. He is a fellow of SPIE and of the Optical Society of America. He served on the SPIE Board of Directors and chairs the SPIE Publications Committee. He also served on the OSA Board of Directors. He served on the National Research Council Committee on Optical Science and Engineering (COSE). His research interests include interferometry and optical testing, optical fabrication, ophthalmic optics, optical measurement systems, optical systems design, and the optics of electronic imaging systems.